University of Montana
ScholarWorks at University of Montana

Graduate Student Theses, Dissertations, & Professional Papers

Graduate School

2022

SENSITIVITY OF LIDAR DERIVED FUEL CELLS TO FIRE MODELING AT LABORATORY SCALE

Anthony Albert Marcozzi
University of Montana

Follow this and additional works at: https://scholarworks.umt.edu/etd

 Part of the Numerical Analysis and Scientific Computing Commons

Let us know how access to this document benefits you.

Recommended Citation

Marcozzi, Anthony Albert, "SENSITIVITY OF LIDAR DERIVED FUEL CELLS TO FIRE MODELING AT LABORATORY SCALE" (2022). *Graduate Student Theses, Dissertations, & Professional Papers*. 11934.
https://scholarworks.umt.edu/etd/11934

This Thesis is brought to you for free and open access by the Graduate School at ScholarWorks at University of Montana. It has been accepted for inclusion in Graduate Student Theses, Dissertations, & Professional Papers by an authorized administrator of ScholarWorks at University of Montana. For more information, please contact scholarworks@mso.umt.edu.

SENSITIVITY OF LIDAR DERIVED FUEL CELLS TO FIRE MODELING AT LABORATORY SCALE

By

ANTHONY MARCOZZI

Bachelor of Science Statistics, University of Missouri, Columbia, MO, 2014

Bachelor of Science Economics, University of Missouri, Columbia, MO, 2014

Bachelor of Science Mathematics, University of Missouri, Columbia, MO, 2014

Master of Science in Computer Science

University of Montana

Missoula, MT

June, 2022

Approved by:

Scott Whittenburg, Dean of The Graduate School

Graduate School

Jesse Johnson, Chair

Computer Science

Douglas Brinkerhoff

Computer Science

Carl Seielstad, Chair

Forestry

Marcozzi, Anthony, M.S., June 2022 Computer Science

Sensitivity of LIDAR Derived Fuel Cells to Fire Modeling at Laboratory Scale

Chairperson: Jesse Johnson

Computational models of wildfires are an important tool for fire managers and scientists. However, fuel inputs to wildfire models can be difficult to represent with sufficient detail to be both computationally efficient and representative of observations. Recent advances in fuel mapping with airborne and terrestrial laser scanning (LIDAR) techniques present new opportunities to capture variation in fuels within a tree canopy and on a landscape. In this paper, we develop a technique for building 3D representations of vegetation from point clouds created by Terrestrial Laser Scans (TLS). Our voxel based approach can be extended to represent heterogeneous crown fuels as collections of fuel cells in modern 3D Computational Fluid Dynamics wildfire models such as FDS, QUIC-Fire, or FIRETEC. We evaluated the effectiveness of our technique at different fuel cell resolutions by using the DAKOTA optimization toolkit to compare simulated fire behavior in FDS with observed burn data collected during a series of experiments at the Missoula Fire Sciences Laboratory. The primary finding was that within the search space of point cloud derived fuel cells, we find accurate descriptions of observed fire behavior with the FDS model. We also find that within our search space, regions of global minima are consistent across fuel cells at different resolutions. This finding suggests that while new techniques are capable of characterizing fuel models with a high degree of fidelity, high resolution 3D fuel models do not improve parity with observed fire behavior in the FDS fire model. The results of this paper offer fire modelers guidelines for translating LIDAR data to 3D fire models, and what fuel cell resolution can best capture accurate fire behavior.

Acknowledgements

I would like to express my sincere gratitude to Jesse Johnson for his advice and wisdom, Carl Seielstad and Doug Brinkerhoff for their feedback and service as committee members, Russ Parsons and the crew at the Missoula Fire Sciences Laboratory for the opportunity to participate in this project, Lucas Wells for his mentorship and lessons in software design, the research team at the University of Montana, and all of my friends and family who made this possible.

Dedicated to my partner Shea, for always inspiring me to be better.

Contents

Chapter 1

Introduction

Computational Fluid Dynamics (CFD) fire models are increasingly used to answer scientific questions related to fire behavior, weather effects, and firefighter safety. While there is debate on the appropriate role of CFD models in scientific and operational modeling [2], there is also increasing interest in overcoming model limitations in order to apply a more general class of coupled fire-atmospheric models to study and manage prescribed fires [14, 15, 23].

Prescribed fire is an important tool for mitigating the threat of wildfire to fire sensitive areas, such as the Wildland Urban Interface [4], as well as achieving landscape goals as a form of wildfire emulation [6]. Physics-based, coupled fire-atmosphere models have been used to simulate grass fires [21, 26], single tree burns [27], and more recently, complex prescribed fire and wildfire environments [23, 11, 28]. However, it is a challenge to describe three-dimensional fuel properties in coupled fire-atmospheric models [23]. Fire modellers must balance trade offs between grid resolution, computational complexity, and data availability to achieve fidelity to limited observations.

This challenge is especially important in light of the important role fuel heterogeneity plays in fire behavior. Laboratory experiments have shown that gaps between shrubs, and the distribution of gaps within an individual shrub, are important factors in determining ignition when exposed to a heat source [38]. Additionally, the distribution of bulk density within a tree canopy was found to significantly alter crown fire potential in a modeled environment [30]. Recent studies have shown that manipulating fuel distributions on a landscape scale through fuel treatments alters

fire behavior in simulations [29, 31, 44]. One study found that increasing fuel fidelity and heterogeneity information impacted fine-scale wind discontinuities which reduced fire spread and area burned [5].

Historically, fuel sampling has been concerned with capturing bulk fuel quantities to support steady state rate of spread fire models such as the Rothermel model [39]. Fuel types were classified through field sampling methods that captured weight per unit area of downed woody material, litter and duff, shrubs, and small conifers [8]. Fuel types capture broad fuel trends on a landscape, but are 2D and overlook vertical fuel heterogeneity in favor of simplifying assumptions.

Advancements in the field of fuel modeling have improved fuel characterization and sampling methods. Recently, fuel sampling methods have been devised in order to capture 3D variability in fine scale fuels [13]. This work offers promising characterizations of fine-scale fuels which drive the behavior of low intensity surface fires often found in prescribed burn environments. However, these techniques are time consuming, labor intensive, and cannot be scaled to stand scale plots.

Another approach to obtaining high fidelity 3D models are point clouds from Terrestrial Laser Scans. TLS has been used to map crown profiles [10], predict canopy fuel loading [41], and simulate 3D surface fuel beds [37]. In addition, point clouds from TLS are capable of generating precision tree models [33] and quantifying vegetative characteristics which can be used with allometric equations for biomass estimates [18]. These techniques are useful for capturing bulk properties of a tree, but do not describe the spatial distribution of vegetative quantities, such as biomass, throughout a tree canopy. Currently, there is no established technique for mapping point clouds to spatially dependent fuel characteristics.

One promising approach to quantifying spatially dependent fuel characteristics is to reduce point cloud complexity by collecting points into bins of gridded voxels. Recent works have successfully modeled mature tree canopies as voxelized point clouds [16, 42]. In addition, voxelized point clouds of fine fuels have been used to measure post-fire consumption [17], and to predict the distribution of mass and 3D structure of shrubs at high resolution [36].

Voxelized point clouds have an additional benefit in that they are a step closer to 3D wildland fuel cells. The fuel cell concept was initially used to describe gridded fuel inputs in a computational domain [7, 9]. The definition was expanded to describe patches of a fuel bed with distinct composition, characteristics, and architecture that become spatially independent beyond $0.5m^2$ [19]. More recently, the concept of a fuel cell has extended to three-dimensions in order to characterize the aggregation of interacting vegetation types [36].

Reducing point clouds to three-dimensional fuel cells is a potentially direct link to gridded fuel inputs for coupled fire-atmospheric models. Such a link would be important because the location, quantity, and characteristics of biomass within a tree canopy are significant factors in determining fire behavior in coupled fire-atmospheric models [27, 30]. Several studies have looked at using combinations of TLS and ALS point clouds to determine the distribution of biomass [17, 36, 41]. To our knowledge no study has attempted to inform the distribution of fuel cells within a 3D CFD fire model using TLS data.

Despite these promising advancements in fire and fuels modeling, there are still significant gaps in the research linking fuel models to the fire modeling environment. Fire modelers must balance careful tradeoffs between computational expense, data collection, and grid resolution when deciding how to represent vegetation as 3D gridded input data. To date, no comparisons have been published between observed fire behavior and simulated fire behavior of LIDAR-derived fuel cells. This paper explores the concept of altering three-dimensional fuel cells in terms of moisture content, bulk density, and resolution to provide an algorithmic approach to translating LIDAR point clouds into a CFD based simulation environment.

Leveraging TLS and mass over time data collected in 2021 on burning saplings at the Missoula Fire Sciences Laboratory, we developed a methodology for representing complex vegetation in three-dimensional fuel cells. Then, we tested the effect of fuel cell descriptors such as fuel moisture content, bulk density, and resolution on modeled fire behavior in the FDS model. We present our methodology, which can be used to translate point cloud data to any CFD fire model with gridded fuel inputs such as FDS, FIRETEC, or QUIC-Fire [25, 20, 22]. Lastly, we provide fire modelers

with heuristics for making decisions on fuel cell fidelity in order to balance simulation accuracy with computational requirements using the FDS model.

Chapter 2

Methods

2.1 Tree Burn Experiments

The sapling burn experiments reported here were conducted in the Missoula Fire Sciences Laboratory burn chamber [35]. The experiment overlapped with ecological work to examine the effect of drought stress on tree mortality when exposed to two controlled levels of fire intensity. We acquired 123 saplings of two species, Engelmann spruce (*Picea engelmannii*) and Ponderosa pine (*Pinus ponderosa*), from a local nursery; 72 were Engelmann spruce and 51 were Ponderosa Pine.

Saplings were acquired in May 2021 and stored in planter containers filled with soil and with roots intact. The trees were stored in a greenhouse from the time of their acquisition until their burn day. During this storage period, half of the saplings from each species were watered every one to two weeks so as to mimic the conditions of a drought environment. The other half were watered every three days so as to

Number of Saplings per Treatment				
Ponderosa Pine	High Heat	Low Heat	No Heat	Total
High Water	8	9	8	25
Low Water	9	8	9	26
Total	17	17	17	51
Engelmann Spruce	High Heat	Low Heat	No Heat	Total
High Water	12	12	12	36
Low Water	12	12	12	36
Total	24	24	24	72

TABLE 2.1: Categorical breakdown of the number of saplings per treatment group.

encourage normal development. Trees in the high water category were watered fully on the day of their burn, regardless of when they had been watered last.

Each day of the experiment, saplings were transported to the burn chamber at the Missoula Fire Sciences Laboratory and ignited over a pair of concentric ring gas burners. During the ignition period, each sapling was exposed to one of three fire intensity categories: no heat treatment, low heat treatment, or high heat treatment. The low heat treatment samples are defined as a flow rate 10.8 liters of propane per minute for a heat release rate per unit area of 516.22 kW/m^2, and the high heat treatment samples are defined as a flow rate 21.6 liters of propane per minute for a heat release rate per unit area of 1032.46 kW/m^2. Table 2.1 lists the number of saplings in each species and treatment category.

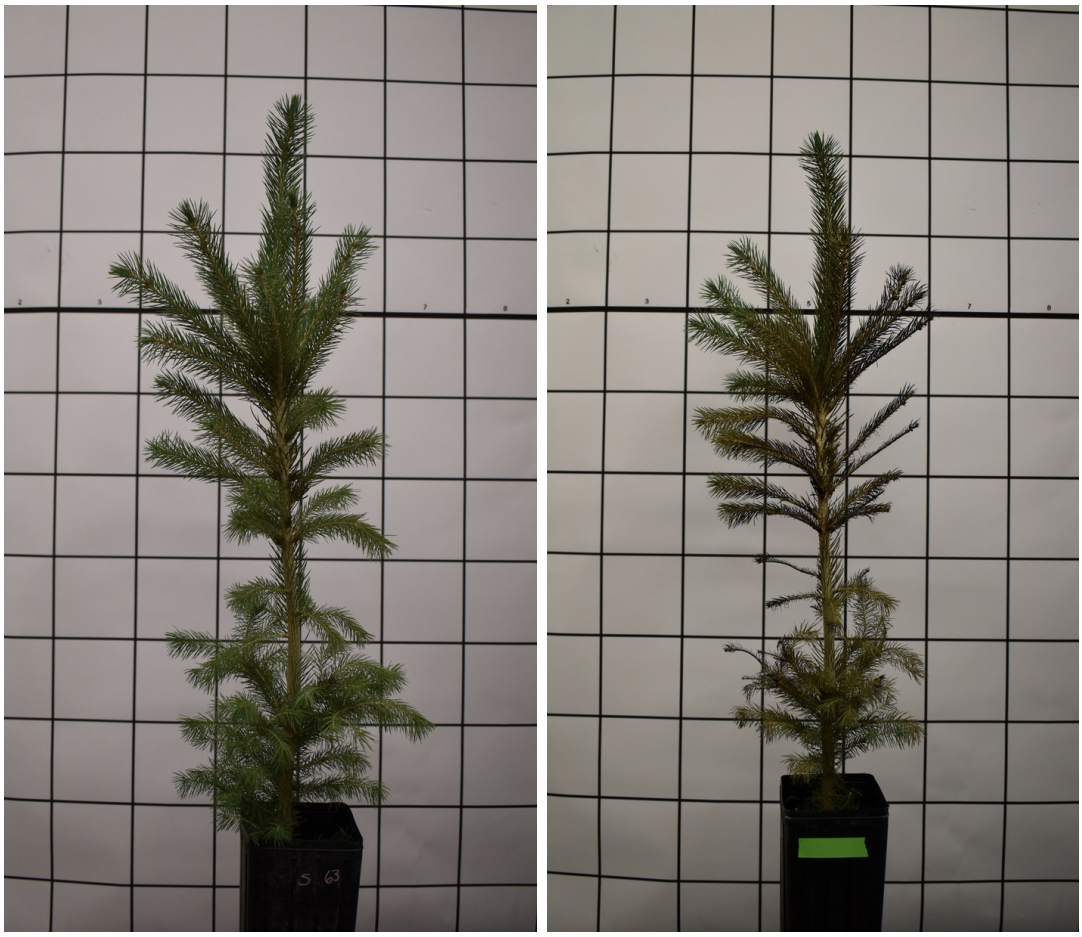

(A) Sapling S63 before heat treatment (B) Sapling S63 after heat treatment

FIGURE 2.1: Comparison pictures of S63 before and after 30 seconds of high heat treatment. S63 was exposed to a high water treatment.

A pair of concentric ring burners were placed over a piece of fibrous cement with a

12.7 cm diameter hole cut in the center. The inner burner ring had a radius of 14.6 cm, and the outer burner ring had a radius of 22.3 cm. Both burners had a width of 1 cm. At the time of the fire treatment, a tree was placed through the hole such that the tree stand rested on a load balance. The height of the apparatus was adjusted to ensure that the crown of each sapling was exposed to the pair of ring ignitors. After ignition, the burner was shut off after 30 seconds. Figure 2.1 compares pictures of an example Engelmann spruce sapling before and after a high heat treatment. This example is a representative sample of the observed burn outcomes for many of the saplings measured in the experiment.

We recorded the weight of the sapling before and after the burning period. Additionally, the weight of the sapling was recorded during the burning period with a load balance transmitting at 0.5 Hz. Figure 2.2 shows a typical set of observations from the load balance over the thirty second burn period for a Ponderosa pine sapling.

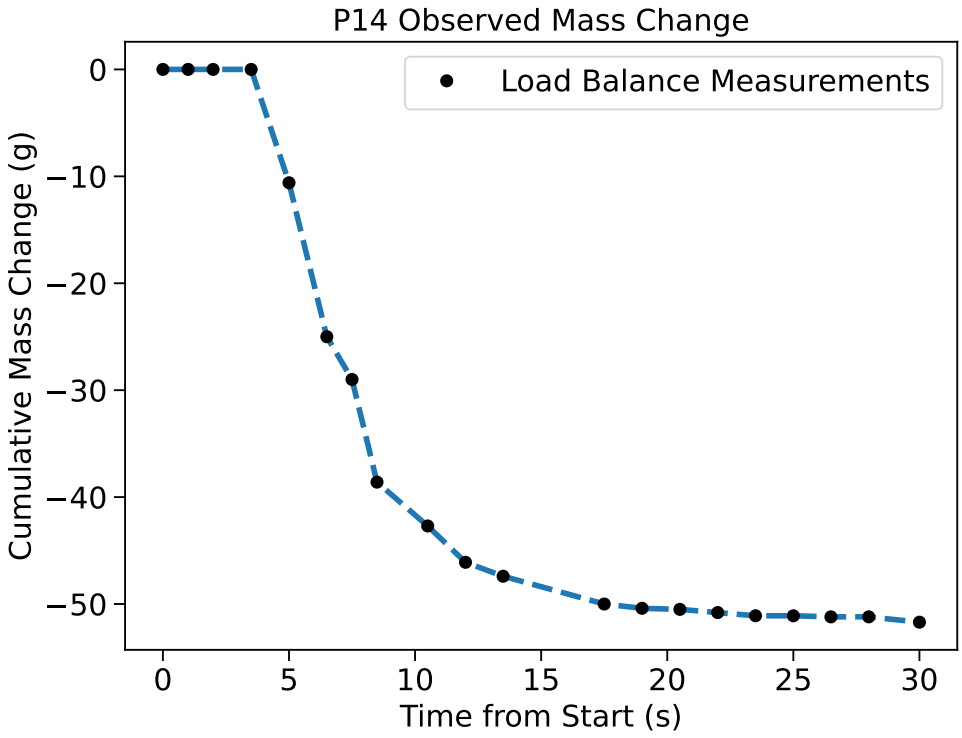

FIGURE 2.2: Cumulative change in mass of a single sapling during a 30 second period of heat exposure from the burner as measured by the load balance.

For each sapling, three-dimensional scans were collected from a Leica Geosystems BLK360 Terrestrial Laser Scanner. The TLS was run at a high density setting with a

reported resolution of 5 mm. Two scans were taken from the same location before and after the burn treatment. Because the scans were taken in the same location, static reference locations in the burn chamber were used to facilitate spatial referencing. The two scans were co-registered using Cyclone Register 360 software from Leica Geosystems in order to create a single 3D point cloud.

In addition, each burn experiment was recorded with an infrared camera and three GoPro cameras. Photographs from four different angles, as well physiological measurements, were taken before and after exposure to the gas burner. Figure 2.3 shows a photograph of the experimental setup with labeled load balance, TLS device, and ring burner.

FIGURE 2.3: Photograph of the experimental design at the Missoula Fire Sciences Laboratory.

2.2 Creating Fuel Cells from a 3D Point Cloud

CFD fire behavior models use volumetric cells (voxels) to represent quantities and spatial distributions of vegetation. In order to represent the point cloud sampling of the physical sapling in a CFD fire behavior model we need to convert the point

cloud into voxels. In this paper, we refer to the combination of the spatial location of a voxel along with its accompanying vegetative quantities as a fuel cell.

In order to translate point cloud data to fuel cells, we begin by reducing the 3D point cloud to a domain containing only point returns within the sapling extent. The colocated TLS point clouds contained points from the entire burn chamber at the Missoula Fire Sciences Laboratory. Points outside the sapling region of interest were removed. Spurious returns were present in the remaining point clouds due to residual ash on the table from previous burns. To account for these superfluous returns, we applied the Point Cloud Outlier Removal tool in the Open3D Python library [43] to filter points farther away from their neighbors compared to the average for the point cloud. Points were filtered more aggressively in the lower third of the sapling to account for a higher accumulation of ash near the burner surface.

There are several challenges associated with correlating 3D point clouds to fine fuel mass and location without the use of destructive sampling. A higher point cloud density does not necessarily correlate to a higher density of foliage or stem biomass. Point density is also related to the scan angle, branch angle, occlusion, and duplicate points from colocated scans [17, 40]. Therefore, there is no known scaling between point density and bulk density.

In order to address the problems related to a 3D point cloud for representing vegetation, we apply a voxelization method to represent collections of points as a single voxel [42]. A voxel based representation of the experimental saplings offers numerous advantages. Duplicated points from stitching multiple scans are represented as a single voxel, voxels can represent points returned to the scanner in addition to points occluded by overlapping woody material, and voxels are one step closer to the concept of a 3D fuel cell necessary for input to a CFD fire model [16].

Our voxelization technique begins by identifying reference voxels. We define a reference voxel as the smallest possible voxel representation of a point cloud, given the physical constraints of the TLS device and the scanning environment. Reference voxels have a Boolean value indicating the presence or absence of points within the

(A) Photograph of S48 (B) Point Cloud Model of S48 (C) Voxel Model of S48

FIGURE 2.4: Comparison between a photograph of spruce sapling 48 (A) and the 3D processed point cloud (B) and reference voxel models (C).

voxel. We chose 1cm x 1cm x 1cm voxels for our reference voxel size due to the reported 5 mm resolution of the TLS device. Smaller reference voxels were attempted, but resulted in grid artifacts due to aliasing. Figure 2.4 compares a photograph of an example spruce sapling with the point cloud and reference voxel models produced by our methodology.

We construct voxels at coarser resolutions by creating a voxel grid in the point cloud domain and counting the number of reference voxels that occur within the voxel at the desired resolution. Thus, when the voxel is converted to a fuel cell, biomass is distributed in proportion to the number of contained reference voxels. This is in contrast to other techniques which distribute vegetative quantities in proportion to the number of point returns. Figure 2.5 shows the relative proportion of reference voxels in a coarse cell. Coarse voxels reduce memory requirements and computational complexity in the context of a CFD fire model. A key part of this study is to compare the results of model output across fuel cell volumes to determine the importance of voxel resolution on modeled fire behavior.

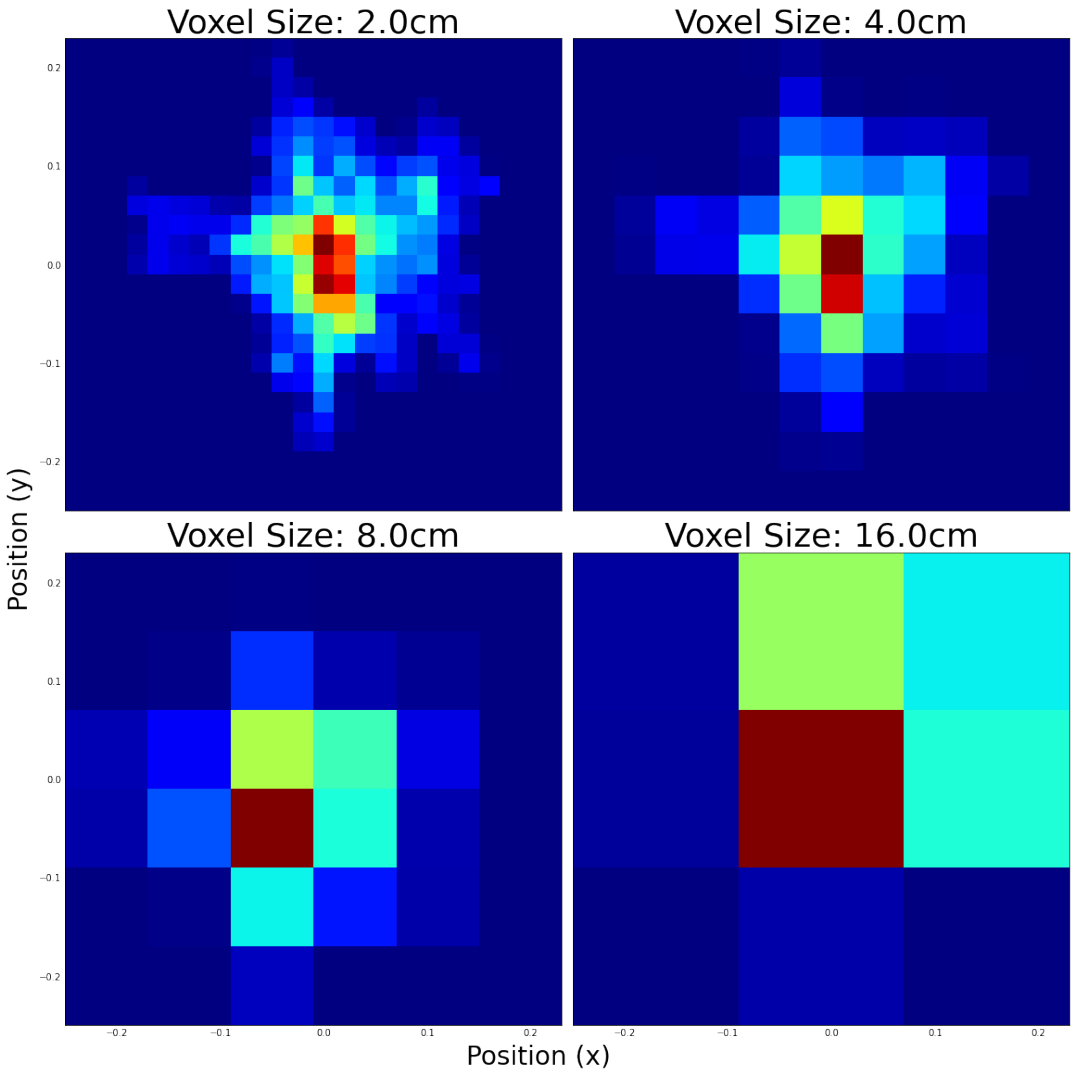

FIGURE 2.5: Distribution of 1cm reference voxels in coarse voxel grids. Each pixel represents the vertical sum of reference voxels across the z-axis. Color is in proportion to the number of reference voxels present within the coarse voxel.

2.3 Fire Behavior Simulation

We compared experimental outcomes with model output from the Fire Dynamics Simulator version 6.7.7 released on November 19th, 2021 [25]. FDS is a computational fluid dynamics (CFD) model of fire-driven fluid flow. The model numerically solves a form of the Navier-Stokes equations appropriate for low-speed, thermally-driven flow, with an emphasis on smoke and heat transport from fires on a rectangular grid. FDS uses a Lagrangian particle model to represent objects that cannot be resolved on the numerical grid. In the particle model, vegetation is represented by a collection of Lagrangian particles that are heated via convection and radiation. Lagrangian particles can be used to represent different types of vegetation like leaves,

grass, and needles that occupy a fuel cell.

Saplings were constructed in FDS as a collection of fuel cells. Fuel cells were spatially distributed in the computational domain using the voxel methodology as discussed in section 2.2. Due to observations from the experimental data, we assume that mass loss was driven by the combustion of foliage. Thus, for our simulation model we distributed biomass to fuel cells in the form of dry foliage mass. Each fuel cell received a quantity of dry foliage mass in proportion to the number of reference voxels contained within the fuel cell. The dry foliage mass, $m_{\text{cell,dry}}$, for a given fuel cell can be computed as:

$$m_{\text{cell,dry}} = m_{\text{ref,dry}} \times n \tag{2.1}$$

Where $m_{\text{ref,dry}}$ is the dry mass of the foliage for a reference voxel, and n is the number of reference voxels contained in the fuel cell.

FDS requires the packing ratio, β, as an input to describe the amount of dry mass represented by the Lagrangian particle in the fuel cell. The packing ratio is a measurement of the compactness of a fuel cell [3]. Another important quantity is the bulk density, ρ_{b}, which represents the dry mass of vegetation per unit volume. For each fuel cell resolution, r, in the n-dimensional point we compute the bulk density of a fuel cell as:

$$\rho_{\text{b}} = \frac{m_{\text{cell,dry}}}{r^3} \tag{2.2}$$

The bulk density is then used to compute the packing ratio for the fuel cell:

$$\beta = \frac{\rho_{\text{b}}}{\rho_{\text{d}}} \tag{2.3}$$

Where particle density, ρ_{d}, is an experimentally determined value representing the density of particles that make up the substance. Particle density differs from the bulk density in that bulk density measures the average density of the substance in a specific medium such as air. We assume that the particle density of needle foliage

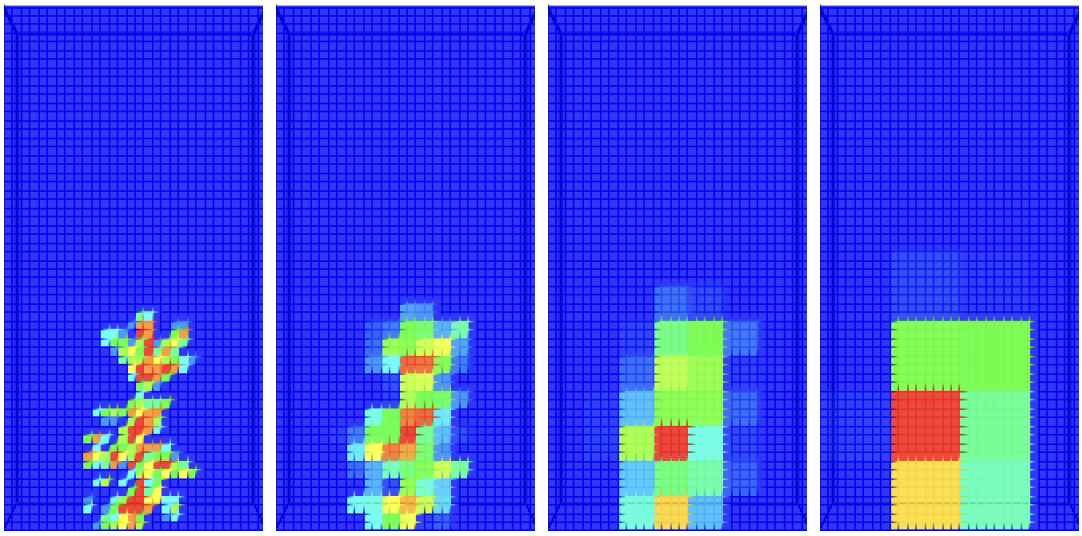

(A) 2cm Fuel Cell (B) 4cm Fuel Cell (C) 8cm Fuel Cell (D) 16cm Fuel Cell

FIGURE 2.6: Distribution of foliage mass in the computational domain for fuel cells of size 2cm (A), 4cm (B), 8cm (C), and 16cm (D).

is 514 kg/m^3 for both the pine and spruce saplings considered [34]. One randomly positioned Lagrangian particle is specified per fuel cell. The amount of foliage a particle represents is determined by the packing ratio of the fuel cell. Figure 2.6 compares the distribution of foliage mass in the FDS domain for an example sapling.

Fuel moisture content is assumed uniform across fuel cells. All other combustion properties are held constant across fuel cells. Model parameters are based on the NIST Douglas Fir experiments in FDS version 6.7.7, and are listed in the FDS Validation Guide [25]. Ignition conditions begin at 0 seconds of simulation time, and mimic the burner treatments used in the experiment. We model the simulation domain on a 0.6m x 0.6m x 1.2m rectangular grid with a cell resolution of 2cm x 2cm x 2cm. We note that the resolution of the rectangular grid in FDS is independent of fuel cell resolution. Fuel cells can have the same, or coarser, resolution as the resolution of the numerical grid. Boundary conditions are open on the sides and top of the domain, and closed at the bottom of the domain. The total mass of the wet foliage fuel element was collected during the 30 seconds of simulated burn activity at 100 Hz.

2.4 Numerical Experiments

We ran computer simulations based on experimental measurements for sixteen of the saplings. For both species we selected two saplings from each drought stress and heat intensity treatment categories. We selected a subset of the total data due to limitations on computational resources. For each of the sixteen saplings in our focus set, we performed a parameter sweep using the DAKOTA toolkit [1]. DAKOTA is a suite of iterative mathematical and statistical methods that can perform parametric exploration of black-box simulations. These parametric explorations can be used for sensitivity analysis, uncertainty quantification, and model calibration.

In our study, we used DAKOTA to perform a multidimensional parameter study, or grid search. We ran the multidimensional parameter study for each of the sixteen focus saplings. Each point in our grid search consisted of three dimensions: dry foliage mass, fuel moisture content, and fuel cell resolution. The dry foliage mass, $m_{\text{total,dry}}$, was uniformly sampled at 16 points over $m_{\text{total,dry}} \in [0.005, 0.08]$kg based on observed mass loss and consumption estimates. Fuel moisture content, M, was uniformly sampled at 16 points over $M \in [20, 350]\%$, following heuristics published in the Fire Behavior Field Reference Guide [12]. Fuel moisture content is computed as the ratio of wet mass to dry mass:

$$M = \frac{m_{\text{total,wet}} - m_{\text{total,dry}}}{m_{\text{total,dry}}} \times 100\% \tag{2.4}$$

Fuel cell resolution, r, was sampled from the set

$$r \in \{2, 4, 8, 16\} \text{ cm}$$

Where each r represents a fuel cell of volume of $r \times r \times r$ cm^3.

A multidimensional parameter study produces a quantifiable response for each parameter set [1]. To find this response, we write the parameters sampled by DAKOTA to an FDS input file in a pre-processing step. This pre-processing step combines the 3D reference voxel fuel model, at the desired fuel cell resolution, with the provided

dry foliage mass and fuel moisture content to populate the FDS domain with fuel cells. Figure 2.6 shows the fuel distributed in the FDS domain at the four considered fuel cell resolutions.

Next, we run a fire behavior simulation using the FDS fire model. FDS produces mass over time data as model output. We quantify the difference between simulated and observed mass loss using Root Mean Square Error.

$$\text{RMSE} = \left(\sum_{i=1}^{N} \frac{(x_i - \hat{x}_i)^2}{N} \right)^{\frac{1}{2}} \tag{2.5}$$

Where N is the number of mass observations, x_i is the observed mass at time step i, and $\hat{x}_i$ is the modeled mass at time step i. The RMSE of a simulation quantifies how close the simulation output matches the observational data. The end result of our numerical experiment is that each set of parameters sampled by DAKOTA has an associated RMSE. Figure 2.7 shows the DAKOTA and FDS pipeline which produces a link between parameters sampled by DAKOTA and RMSE.

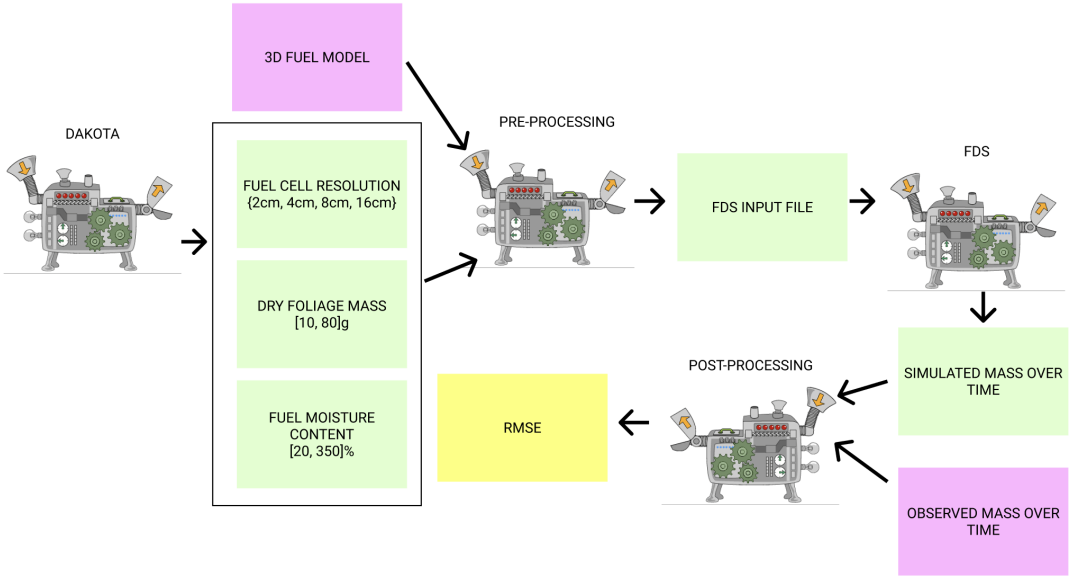

FIGURE 2.7: Outline of the workflow between DAKOTA and FDS. This cycle is run for all 16,384 points in the multidimensional parameter study. The workflow produces a direct link between parameters sampled by DAKOTA and a measure of goodness of fit between simulation output and observed data.

Chapter 3

Results

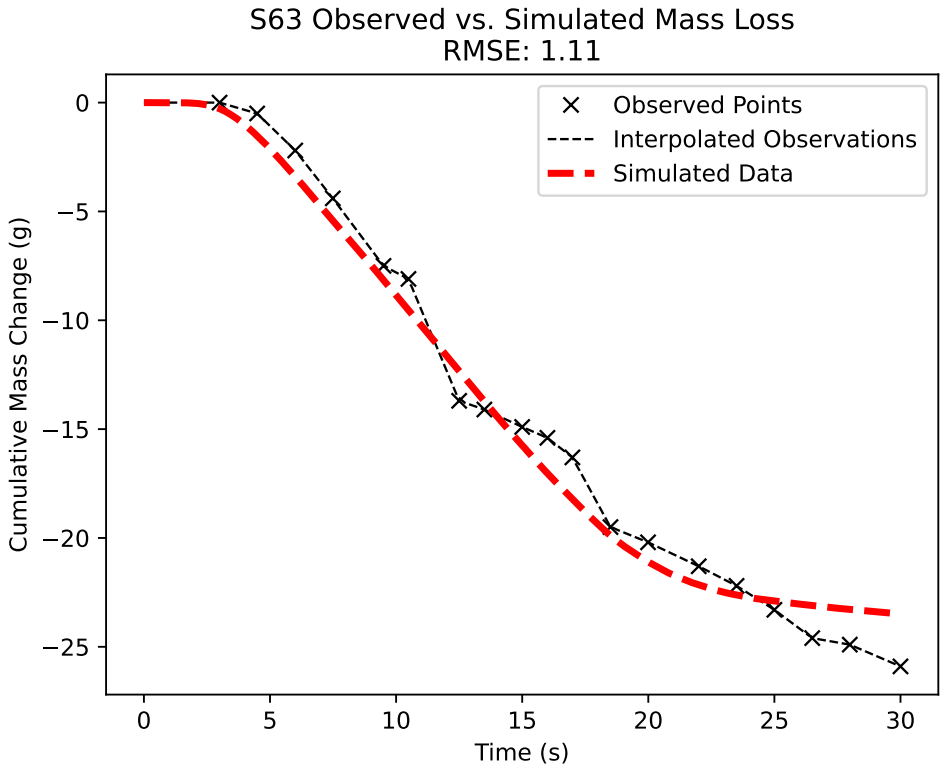

FIGURE 3.1: Comparison between simulated and observed curves of cumulative mass change. The red line shows the cumulative change in mass from the FDS fire model, whereas the black line with x marks shows the observed cumulative mas change as measured by the load balance for sapling S63. This is the lowest RMSE value found out of the 16,384 model runs.

We computed the RMSE of each simulation in the parameter sweep across sixteen saplings. For each sapling, we found the minimum RMSE determined from comparing the mass loss curves for observed and simulated burns. Figure 3.1 shows the minimum RMSE found in the set of simulations for Engelmann spruce sapling S63. We observe close parity between the simulated and observed mass loss in both

the shape of the curves and the resulting change in mass. However, the simulated mass loss curve captures a smooth, sigmoidal relationship between cumulative mass change and time. It does not capture the plateaus and variable drops in cumulative mass change found in the observed mass loss curve.

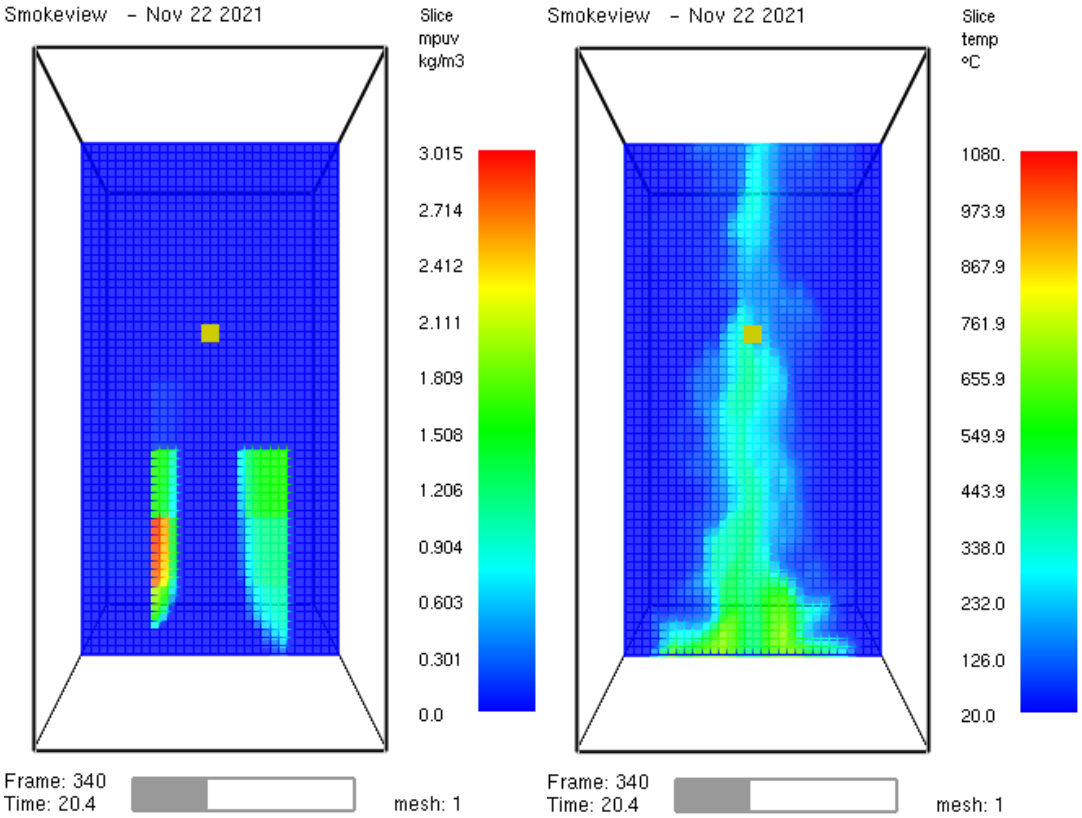

(A) Mass per Unit Volume kg/m^3 (B) Cell-centered Temperature °C

FIGURE 3.2: Smokeview views of mass per unit volume (A) and cell-centered temperature (B) at simulation time 20.4 seconds in an example FDS simulation.

Despite the close relationship between observed and simulated mass loss curves in Figure 3.1, we also observe non-physical fire behavior in the FDS model. Figure 3.2 shows non-physical fire behavior present in an example FDS simulation. In this simulation, the primary area of consumption is the center of the simulated sapling along the central axis. For reference, Figure 2.6d shows the initial distribution of foliage mass in the simulation. This modeled behavior contradicts observed fire effects in the experimental data. Figure 2.1 suggests that most of the combustion of foliage occurred away from the stem of the sapling, whereas the model suggests the opposite. We also find that the central concentration of simulated temperature differs from experimental data which show an even temperature distribution.

The correspondence between RMSE and the independent variables allows us to examine the space sampled by DAKOTA in our multidimensional parameter study. Figure 3.3 shows the results of the numerical experiment as described above for one Engelmann spruce sapling. Each pane in the image represents a parameter sweep across 2D points for a given fuel cell resolution. Each pixel has a value for fuel moisture content and dry foliage mass. Fuel moisture content was sampled uniformly in the range [20, 350]%, and dry foliage mass was sampled in the range [10, 80]g for a total of 256 points for each sampled fuel cell resolution.

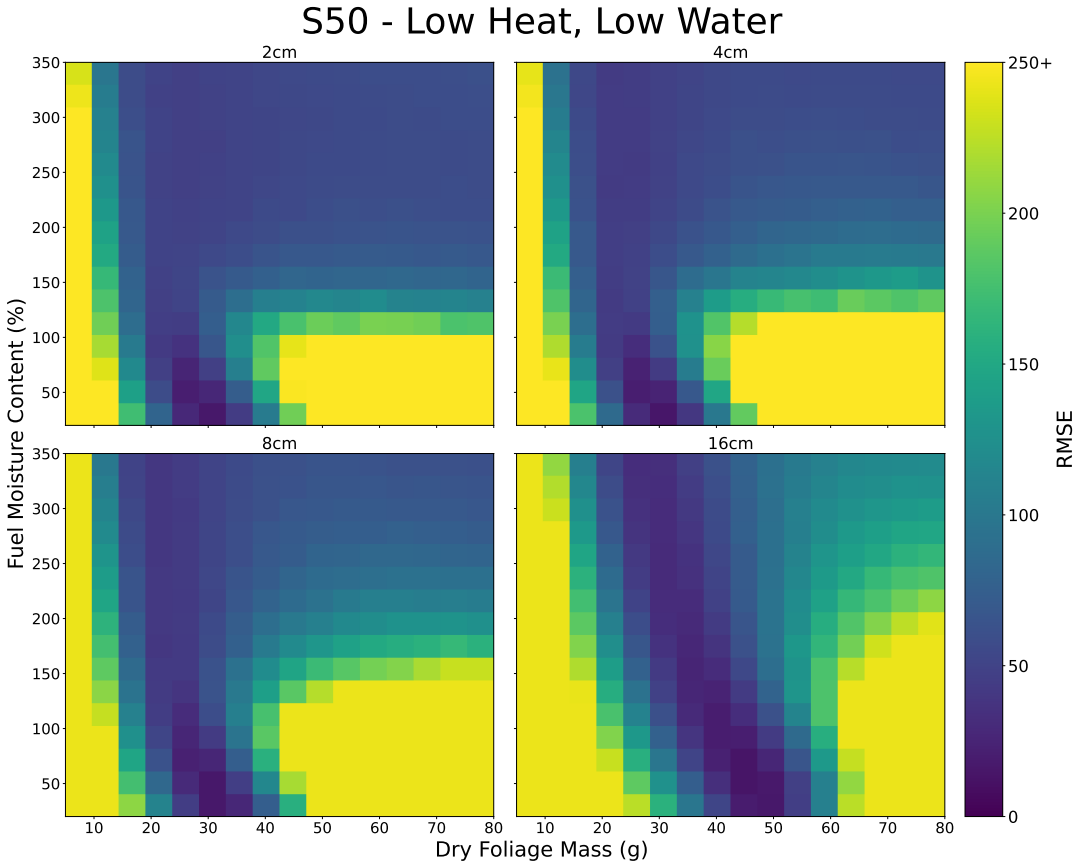

FIGURE 3.3: Distribution of RMSE values for the full 1,024 samples in the parameter sweep for sapling S50. The upper left pane is for simulations with a fuel cell resolution of 2cm, upper right for 4cm, bottom left for 8cm, and bottom right for 16cm. The x and y axis of each pane correspond to the sampled range of dry foliage mass and fuel moisture content. Each pixel is colored according to the RMSE resulting from the comparison between the simulated model output and the observed data for sapling S50.

The multidimensional parameter study identifies a region of consistent minima across all fuel cell resolutions. The model is sensitive to dry foliage mass values as evidenced by the areas of high RMSE below 25g and above 50g along the x-axis in figure 3.3. Minimum RMSE values occur at higher dry foliage mass values for the coarsest

fuel cell resolution of 16cm x 16cm x 16cm. Additionally, the model shows sensitivity to fuel moisture content. This effect is more pronounced when dry foliage mass is high, and the model appears less sensitive to fuel moisture content when the dry foliage mass is low. The parameter sweep identifies a consistent region of minima across all fuel cell resolutions. We find that the coarsest fuel cell resolution expands the area of RMSE minima across a larger range of dry foliage mass values.

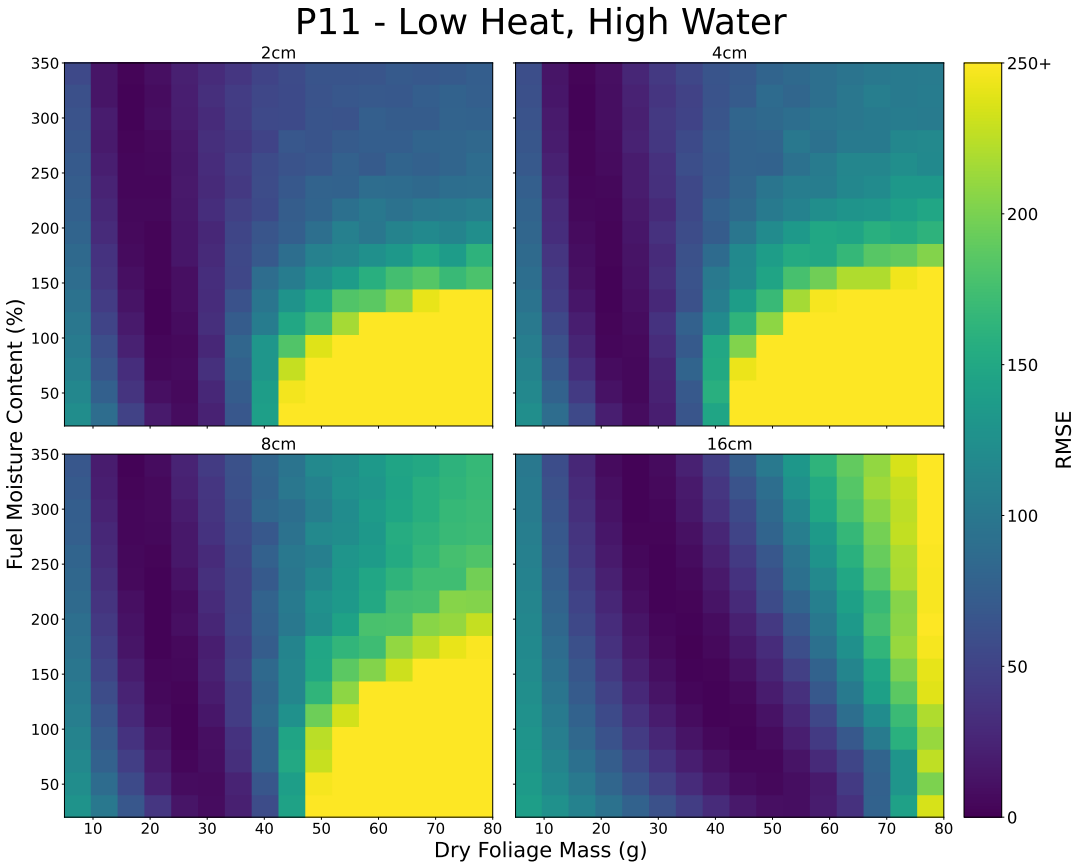

FIGURE 3.4: Distribution of RMSE values for the full 1,024 samples in the parameter sweep for sapling P11. The upper left pane is for simulations with a fuel cell resolution of 2cm, upper right for 4cm, bottom left for 8cm, and bottom right for 16cm. The x and y axis of each pane correspond to the sampled range of dry foliage mass and fuel moisture content. Each pixel is colored according to the RMSE resulting from the comparison between the simulated model output and the observed data for sapling P11.

Figure 3.4 shows a similar parameter space plot as discussed above for a Ponderosa pine sapling that received a low heat treatment and a high water treatment during the experiment. Once again, we observe areas of minima across all fuel cell resolutions. The cost surface of the coarsest 16cm fuel cell resolution deviates significantly from the finer fuel cell resolutions. We also observe parity between a low dry foliage

mass and high fuel moisture content, and a high dry foliage mass and low fuel moisture content. For example, in the 4cm fuel cell resolution pane, the RMSE associate with a dry foliage mass of 25g and 50% fuel moisture content is roughly equivalent to the RMSE associated with a dry foliage mass of 20g and a fuel moisture content of 350%.

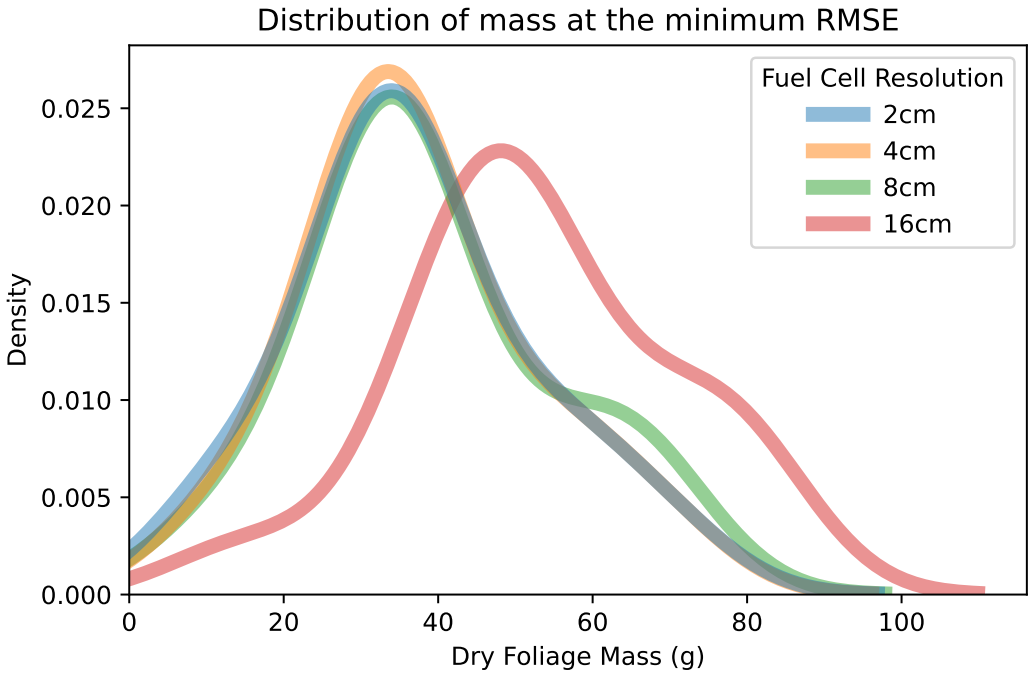

FIGURE 3.5: Kernel density estimate plots of the dry foliage mass associated with the minimum RMSE for each fuel cell and n=16 saplings. The distribution of dry foliage mass is plotted as an individual curve for each fuel cell.

While we observe areas of minima across fuel cell resolutions in the parameter sweep, the area of minima shifts with respect to dry foliage mass in the coarsest resolution considered. Figure 3.5 shows kernel density estimates computed over the dry foliage mass value at the lowest RMSE simulation for each fuel cell resolution. Density estimates for the 2, 4, and 8cm fuel resolution simulations suggest close parity. However, the coarsest fuel cell shows a distinct rightward shift of the density plot with respect to dry foliage mass. We find a mean minimum RMSE dry foliage mass of 37.92g with a standard deviation of 15.33g for the 2-8cm fuel cell resolutions, and a mean of 52.81g with a standard deviation of 17.32g for the coarsest fuel cell resolution.

In addition to the parameter space plots for individual saplings, we also analyze the

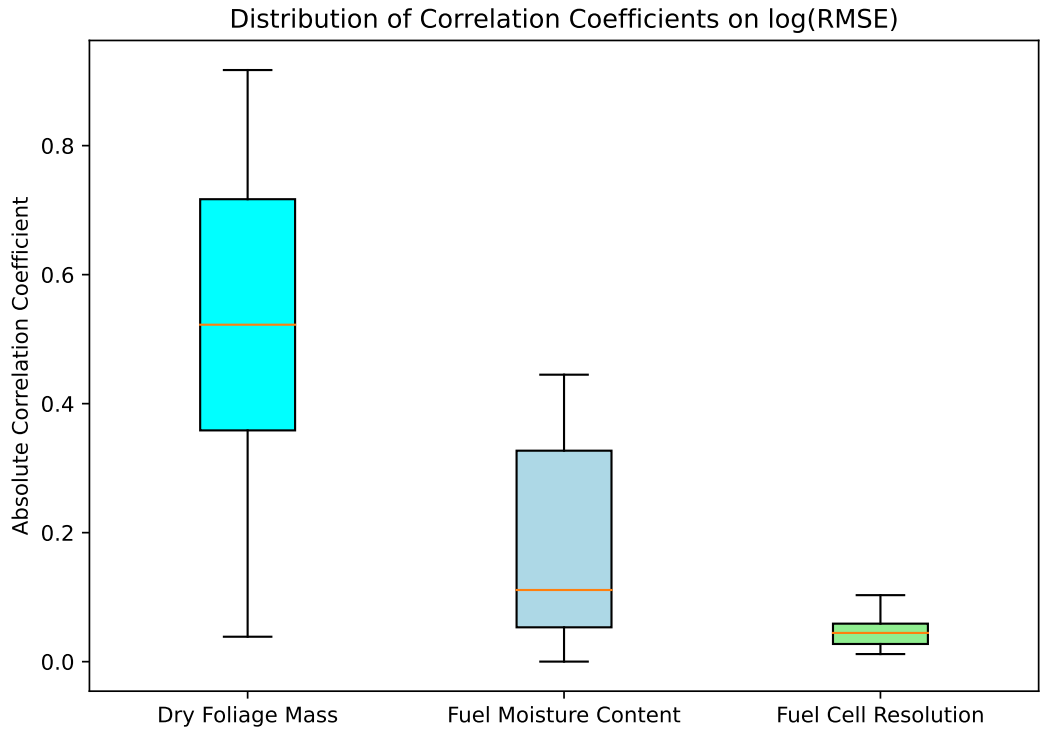

FIGURE 3.6: Box and whisker plot of the distribution of correlation coefficients between log(RMSE) and three independent variables: Dry Foliage Mass, Fuel Moisture Content, and Fuel Cell Resolution for n=16 saplings. The box extends from the first quartile (Q1) to the third quartile (Q3) of the data, with a line at the median. Whiskers extend from the lowest correlation coefficient to the highest correlation coefficient in the data. We take the absolute value of the correlation coefficient in order to capture the magnitude, but not the direction, of the correlation.

effects of independent variables on RMSE. We compute the Pearson correlation coefficients between dry foliage mass, fuel moisture content, and fuel cell resolution on the logarithm of RMSE for each of the sixteen multidimensional parameter studies. The distribution of correlation coefficients are displayed in Figure 3.6. This result suggests that fuel cell resolution has a significantly lower ability to predict RMSE than dry foliage mass or fuel moisture content.

The correlation coefficients for dry foliage mass and fuel moisture content are likely underestimated due to the non-monotonic behavior of the RMSE values. Such non-monotonic behavior can be observed, for example, in the valleys of minima that occur along the x-axis of figure 3.3. This analysis is meant to illustrate the relative importance of dry foliage mass and fuel moisture content for predicting RMSE.

Chapter 4

Discussion

In this study we developed a methodology for describing heterogeneous canopy fuel loads using LIDAR point clouds. Next, we conducted a series of numerical experiments examining the effectiveness of this technique by comparing FDS model output with observed load balance data taken from a series of experimental tree burns. We used DAKOTA to conduct a parameter sweep on fuel moisture content and dry foliage mass and identified physically plausible local minima. Additionally, we found that our sampling technique identified an area of RMSE minima for all fuel cell resolutions, and that the area was consistent for 2-8cm resolution fuel cells.

Our work presented here represents a shift from traditional approaches for modeling fuels in CFD fire models. Previous works have used simplified geometries like cones or cylinders with homogeneous and continuous fuel distributions to model fire behavior in individual trees [27] and stands [31]. However, it is well documented that heterogeneous fuel distributions have a large impact on fire behavior [30, 32]. While other studies have built systems for deriving fuel models from LIDAR point clouds [24, 37], our study is the first that we are aware of to make a direct link between LIDAR point clouds and fuel inputs to 3D fire effects models.

Enhanced models of fuel derived from LIDAR data have the potential to link advanced fire behavior models with field observations [14]. For example, such a process opens the door to collecting LIDAR data in fire sensitive areas to assess the impact of a hypothetical fire disturbance. In addition, the capability to quantify variability in fuels on a landscape presents opportunities to evaluate the effectiveness of management actions like prescribed burns or fuel treatments.

Our fuel cell methodology represents a first step at achieving this goal of linking data from LIDAR points clouds and coupled fire-atmospheric models. While we found close parity between our fire simulations in FDS and observational data using our 3D fuel models, many opportunities for further research and refinement exist. For example, our technique tends to over-sample reference voxels associated with the stem of the saplings. The result of this phenomenon is the over-weighting of combustible thermally thin foliage concentrated in the middle of the 3D fuel model. This phenomenon is well represented in Figure 2.5, and likely results in an overestimation of mass loss when the vegetation is exposed to a heat source in a fire effects model. Future research can expand on previous work segmenting foliage from woody material in LIDAR point clouds [40] in order improve our methodology by characterizing reference voxels by vegetative return type.

In our numerical experiment, we link observations of fire behavior, data from LIDAR point clouds, and fire effects from the FDS model. We accomplish this by comparing model output with observed mass loss data. We used DAKOTA to uniformly sample the parameter space of dry foliage mass, fuel moisture content, and fuel cell resolution for sixteen saplings. This experiment also has implications for fire behavior modeling. One important modeling conclusion that we draw from our results is the relative importance of dry foliage mass and fuel moisture content on predicting mass loss. Fuel cell resolution was found to have little impact on the characterization of modeled mass loss, whereas dry foliage mass and fuel moisture content were found to be highly correlated with characterizing observed mass loss.

Both fine and coarse fuel cell grids were capable of accurately characterizing observed mass loss in a simulation environment. Based on these results, we conclude that if the primary goal of a simulation is to reproduce the burning behavior of a 3D fuel model, then a coarse fuel cell grid can successfully balance tradeoffs between computational complexity and representative heterogeneity. While high resolution LIDAR data can improve the representative heterogeneity of 3D fuel models, we find that high resolution fuel descriptions do not improve model results.

Additionally, the importance of dry foliage mass and fuel moisture content suggest that fire modelers should have a high level of confidence in their fuel attributes in

order to have confidence in model results. Non-destructive biomass estimates of vegetation are an active area of research. Our study suggests that obtaining accurate biomass estimates is crucial for achieving model accuracy. More work is needed to examine the relationship between biomass measurements from traditional field techniques or derived from LIDAR data, and fuel inputs to couple fire-atmospheric models.

One major shortcoming of our study is that we were unable to evaluate the relationship between numerically identified fuel attributes from RMSE minima and actual fuel attributes measured from vegetation samples. While the majority of parameter spaces resulted in physically plausible fuel attributes, regions of RMSE minima also contained physically implausible minima. For example, our numerical experiments consistently identified regions of high dry foliage mass and low fuel moisture content as minima. This often contradicted known high water treatments applied to the sapling.

The tendency for the core of the simulated sapling to burn, as seen in Figure 3.2a, may be responsible for pushing RMSE minima out of the range of physically plausible values. This phenomenon likely occurs for two reasons. Firstly, the closed boundary condition at the bottom of the simulated domain contributes to a strong air draw along the central axis. This concentrates the energy introduced by the burner to the middle of the sapling which can be seen in Figure 3.2b. Secondly, the central axis of the simulation domain is over-weighted with fuel cells associated with the stem of the sapling. Due to these two factors, our study likely overestimates the role that the combustion of thermally thin vegetation plays in driving mass loss.

Future research can examine the role of branchwood in thermal degradation, velocity fields, and moisture content. The role of DAKOTA can expand to include additional parameters, simulation designs, and more advanced analysis techniques. Additional investigations into the effects of more detailed 3D fuel models on fire behavior models will help us better understand how to apply coupled fire-atmospheric fire models to real world problems like prescribed burn planning.

Bibliography

[1] B. Adams, W. Bohnhoff, K. Dalbey, M. Ebeida, J. Eddy, M. Eldred, R. Hooper, P. Hough, K. Hu, J. Jakeman, M. Khalil, K. Maupin, J. A. Monschke, E. Ridgway, A. Rushdi, D. Seidl, J. Stephens, and J. Winokur. Dakota, a multilevel parallel object-oriented framework for design optimization, parameter estimation, uncertainty quantification, and sensitivity analysis: Version 6.15 user's manual. *Sandia Technical Report SAND2020-12495*, November 2021.

[2] M. E. Alexander and M. G. Cruz. Are the applications of wildland fire behaviour models getting ahead of their evaluation again? *Environmental Modelling and Software*, 41:65–71, mar 2013.

[3] P. L. Andrews. The rothermel surface fire spread model and associated developments: A comprehensive explanation. *USDA Forest Service - General Technical Report RMRS-GTR*, 2018(371):1–121, 2018.

[4] S. F. Arno and J. K. Brown. Overcoming the paradox in managing wildland fire. *Western Wildlands*, (17):40–46, 1991.

[5] A. L. Atchley, R. Linn, A. Jonko, C. Hoffman, J. D. Hyman, F. Pimont, C. Sieg, and R. S. Middleton. Effects of fuel spatial distribution on wildland fire behaviour. *International Journal of Wildland Fire*, 30(3):179–189, jan 2021.

[6] W. L. Baker. *Fire Ecology in Rocky Mountain Landscapes*. Island Press, 2009.

[7] J. K. Brown. Bulk Densities of Nonuniform Surface Fuels and their Application to Fire Modeling. *Forest Science*, 27(4):667–683, 1981.

[8] J. K. Brown, R. D. Oberheu, and C. M. Johnston. Handbook for inventorying surface fuels and biomass in the interior West. Technical report, 1982.

[9] E. A. Catchpole, T. J. Hatton, and W. R. Catchpole. Fire spread through non-homogeneous fuel modelled as a Markov process. *Ecological Modelling*, 48(1-2):101–112, oct 1989.

[10] J. Ferrarese, D. Affleck, and C. Seielstad. Conifer crown profile models from terrestrial laser scanning. *Silva Fennica*, 49(1), 2015.

[11] M. R. Gallagher, Z. Cope, D. R. Giron, N. S. Skowronski, T. Raynor, T. Gerber, R. R. Linn, and J. K. Hiers. Reconstruction of the spring hill wildfire and exploration of alternate management scenarios using quic-fire. *Fire*, 4(4):72, oct 2021.

[12] N. W. C. Group. Fire behavior field reference guide. pms-437. *National Wildfire Coordination Group*, July 2014.

[13] C. M. Hawley, E. L. Loudermilk, E. M. Rowell, and S. Pokswinski. A novel approach to fuel biomass sampling for 3D fuel characterization. *MethodsX*, 5:1597–1604, jan 2018.

[14] J. K. Hiers, J. J. O'Brien, J. M. Varner, B. W. Butler, M. Dickinson, J. Furman, M. Gallagher, D. Godwin, S. L. Goodrick, S. M. Hood, A. Hudak, L. N. Kobziar, R. Linn, E. L. Loudermilk, S. McCaffrey, K. Robertson, E. M. Rowell, N. Skowronski, A. C. Watts, and K. M. Yedinak. Prescribed fire science: the case for a refined research agenda. *Fire Ecology*, 16(1), dec 2020.

[15] C. M. Hoffman, C. H. Sieg, R. R. Linn, W. Mell, R. A. Parsons, J. P. Ziegler, and J. K. Hiers. Advancing the science of wildland fire dynamics using process-based models. *Fire*, 1(2):1–6, sep 2018.

[16] F. Hosoi and K. Omasa. Voxel-based 3-D modeling of individual trees for estimating leaf area density using high-resolution portable scanning lidar. *IEEE Transactions on Geoscience and Remote Sensing*, 44(12):3610–3618, 2006.

[17] A. T. Hudak, A. Kato, B. C. Bright, E. L. Loudermilk, C. Hawley, J. C. Restaino, R. D. Ottmar, G. A. Prata, C. Cabo, S. J. Prichard, E. M. Rowell, and D. R. Weise. Towards Spatially Explicit Quantification of Pre- A nd Postfire Fuels and Fuel

Consumption from Traditional and Point Cloud Measurements. *Forest Science*, 66(4):428–442, aug 2020.

[18] S. Kaasalainen, A. Krooks, J. Liski, P. Raumonen, H. Kaartinen, M. Kaasalainen, E. Puttonen, K. Anttila, and R. Mäkipää. Change Detection of Tree Biomass with Terrestrial Laser Scanning and Quantitative Structure Modelling. *Remote Sensing 2014, Vol. 6, Pages 3906-3922*, 6(5):3906–3922, apr 2014.

[19] J. A. Kevin Hiers, J. J. O, R. J. Mitchell A, J. M. Grego C, and E. D. Louise Loudermilk A Joseph W Jones. The wildland fuel cell concept: an approach to characterize fine-scale variation in fuels and fire in frequently burned longleaf pine forests. *International Journal of Wildland Fire18: 315–325*, 18:315–325, 2009.

[20] R. Linn, J. Reisner, J. J. Colman, and J. Winterkamp. Studying wildfire behavior using FIRETEC. *International Journal of Wildland Fire*, 11(3-4):233–246, 2002.

[21] R. R. Linn and P. Cunningham. Numerical simulations of grass fires using a coupled atmosphere-fire model: Basic fire behavior and dependence on wind speed. *Journal of Geophysical Research Atmospheres*, 110(13):13107, 2005.

[22] R. R. Linn, S. L. Goodrick, S. Brambilla, M. J. Brown, R. S. Middleton, J. J. O'Brien, and J. K. Hiers. QUIC-fire: A fast-running simulation tool for prescribed fire planning. *Environmental Modelling and Software*, 125:104616, mar 2020.

[23] R. R. Linn, J. L. Winterkamp, J. H. Furman, B. Williams, J. K. Hiers, A. Jonko, J. J. O'brien, K. M. Yedinak, and S. Goodrick. Modeling low intensity fires: Lessons learned from 2012 rxcadre. *Atmosphere*, 12(2):1–19, jan 2021.

[24] E. L. Loudermilk, J. K. Hiers, J. J. O'Brien, R. J. Mitchell, A. Singhania, J. C. Fernandez, W. P. Cropper, and K. C. Slatton. Ground-based LIDAR: A novel approach to quantify fine-scale fuelbed characteristics. *International Journal of Wildland Fire*, 18(6):676–685, sep 2009.

[25] K. McGrattan, R. McDermott, C. Weinschenk, and G. Forney. *Fire Dynamics Simulator Users Guide, Sixth Edition*. Special Publication (NIST SP), National Institute of Standards and Technology, Gaithersburg, MD, November 2013.

[26] W. Mell, M. A. Jenkins, J. Gould, and P. Cheney. A physics-based approach to modelling grassland fires. *International Journal of Wildland Fire*, 16(1):1–22, 2007.

[27] W. Mell, A. Maranghides, R. McDermott, and S. L. Manzello. Numerical simulation and experiments of burning douglas fir trees. *Combustion and Flame*, 156(10):2023–2041, oct 2009.

[28] E. V. Mueller, N. S. Skowronski, K. L. Clark, M. R. Gallagher, W. E. Mell, A. Simeoni, and R. M. Hadden. Detailed physical modeling of wildland fire dynamics at field scale - An experimentally informed evaluation. *Fire Safety Journal*, 120:103051, 2021.

[29] R. Parsons, R. Linn, F. Pimont, C. Hoffman, J. Sauer, J. Winterkamp, C. Sieg, and W. Jolly. Numerical Investigation of Aggregated Fuel Spatial Pattern Impacts on Fire Behavior. *Land*, 6(2):43, jun 2017.

[30] R. A. Parsons, W. E. Mell, and P. McCauley. Linking 3D spatial models of fuels and fire: Effects of spatial heterogeneity on fire behavior. *Ecological Modelling*, 222(3):679–691, feb 2011.

[31] R. A. Parsons, F. Pimont, L. Wells, G. Cohn, W. M. Jolly, F. de Coligny, E. Rigolot, J. L. Dupuy, W. Mell, and R. R. Linn. Modeling thinning effects on fire behavior with STANDFIRE. *Annals of Forest Science*, 75(1), 2018.

[32] F. Pimont, J. L. Dupuy, R. R. Linn, and S. Dupont. Validation of FIRETEC wind-flows over a canopy and a fuel-break. *International Journal of Wildland Fire*, 18(7):775–790, oct 2009.

[33] P. Raumonen, M. Kaasalainen, Å. Markku, S. Kaasalainen, H. Kaartinen, M. Vastaranta, M. Holopainen, M. Disney, and P. Lewis. Fast Automatic Precision Tree Models from Terrestrial Laser Scanner Data. *Remote Sensing 2013, Vol. 5, Pages 491-520*, 5(2):491–520, jan 2013.

[34] S. Ritchie, K. Steckler, A. Hamins, T. Cleary, J. Yang, and T. Kashiwagi. The Effect Of Sample Size On The Heat Release Rate Of Charring Materials, 1997.

[35] R. C. Rothermel. A mathematical model for predicting fire spread in wildland fuels. Technical report, (Forest Service - Rocky Mountain Research Station),

1972.

[36] E. Rowell, E. L. Loudermilk, C. Hawley, S. Pokswinski, C. Seielstad, L. L. Queen, J. J. O'Brien, A. T. Hudak, S. Goodrick, and J. K. Hiers. Coupling terrestrial laser scanning with 3D fuel biomass sampling for advancing wildland fuels characterization. *Forest Ecology and Management*, 462:117945, apr 2020.

[37] E. Rowell, E. L. Loudermilk, C. Seielstad, and J. J. O'Brien. Using Simulated 3D Surface Fuelbeds and Terrestrial Laser Scan Data to Develop Inputs to Fire Behavior Models. *Canadian Journal of Remote Sensing*, 42(5):443–459, sep 2016.

[38] L. Schneider, B. Betting, M. Patterson, N. Skowronski, and A. Simeoni. Experimental study of fire spread through discontinuous fuels without flame contact. *Fire Safety Journal*, 120:103066, may 2021.

[39] J. H. Scott and R. E. Burgan. Standard fire behavior fuel models: A comprehensive set for use with Rothermel's surface fire spread model. *USDA Forest Service - General Technical Report RMRS-GTR*, (153 RMRS-GTR):1–76, 2005.

[40] C. Seielstad, C. Stonesifer, E. Rowell, and L. Queen. Deriving fuel mass by size class in Douglas-fir (Pseudotsuga menziesii) using terrestrial laser scanning. *Remote Sensing*, 3(8):1691–1709, aug 2011.

[41] N. S. Skowronski, K. L. Clark, M. Duveneck, and J. Hom. Three-dimensional canopy fuel loading predicted using upward and downward sensing LiDAR systems. *Remote Sensing of Environment*, 115(2):703–714, 2011.

[42] J. Stoker. Volumetric visualization of multiple-return lidar data: Using voxels. *Photogrammetric Engineering and Remote Sensing*, 75(2):109–112, 2009.

[43] Q.-Y. Zhou, J. Park, and V. Koltun. Open3D: A Modern Library for 3D Data Processing. *arXiv preprint arXiv:1801.09847*, jan 2018.

[44] J. P. Ziegler, C. Hoffman, M. Battaglia, and W. Mell. Spatially explicit measurements of forest structure and fire behavior following restoration treatments in dry forests. *Forest Ecology and Management*, 386:1–12, feb 2017.